Application Potential of Pnp-Switching Semiconductors

Philipp Deng,[a] Matthias Hoffmann,[a] and Tom Nilges*[a]

Dedicated to Prof. Dr. Dr. h. c. Hubert Schmidbauer on the occasion of his 90th birthday

Materials with tunable properties are often in the focus of materials science. Up to this point four different semiconducting materials and substitution variants have been found that are capable of switching between p- and n-type conduction by a simple change in temperature. In this review, we illustrate previous findings of these pnp-switching materials and current developments in functional implementations. While in the past decade, the scientific focus was primarily on discovering new materials that possess this intriguing switching effect, recently the first devices were successfully constructed and tested. Using the compounds, $Ag_{18}Cu_3Te_{11}Cl_3$ and AgCuS, that exhibit the pnp-switching behaviour at approximately room temperature and 364 K, respectively, two single-material diodes were developed and characterized. The approach for inducing this effect is denoted and the fundamental principles for realizing these devices are summarized.

1. Introduction

P- and n-doped semiconductors are used in manifold applications ranging from catalysis, IT technology and energy conversion processes. Negatively-charged electrons and positively-charged holes are dominant charge carriers in such materials. In many catalytic reactions semiconductors are utilized to deliver charge carriers with the right energy to accelerate redox reactions in water splitting or photocatalytic processes.[1] Contacting n- and p-type semiconductors electronically lead to prominent pn-diodes and npn/pnp-transistors which are integral units in modern computer and IT technology.[2] The semiconductor type is addressed and created by suitable doping processes in a given semiconducting compound. The control of the semiconductor type is crucial for any of the aforementioned processes. Devices are produced by controlled deposition and generation of n- and p-type semiconducting areas.[3] Semiconductors that exhibit collective structural rearrangements, electronic or spin structure modulations, or phonon dispersion effects often have interesting physical properties like superionic conduction, superconductivity, giant magnetocaloric or resistance effects, or improved thermoelectric properties.[4]

The pnp-switch located in a single compound, as present in all materials discussed in this review article, is an intriguing property because p- and n-type conduction can be addressed and adjusted by a simple external stimulus, the temperature.

Consequently, these materials do not require doping to generate either a p- or n-type semiconductor anymore and only the control of temperature is needed to select the type of conduction. This offers a plethora of possible applications once this effect can be applied to processes where either electrons or holes play a crucial role.

Discovered in 2009, $Ag_{10}Te_4Br_3$ was the very first compound capable of switching reversibly between p-type and n-type conduction during a structural phase transition at 390 K induced merely by temperature change.[5] No extrinsic doping with other elements is necessary to change the semiconducting mechanism. Since this discovery, a systematic search for other pnp-switching compounds was started, resulting in reports on four additional materials in the subsequent years that show this intriguing effect.

The second compound reported by Xie et al. in 2012 was $AgBiSe_2$. Here, a reasonably high thermoelectric performance (ZT 1.5 at 700 K) and a pnp-switch at 580 K, which is caused by an Ag/Bi exchange during a reversible structural phase transition, is observed. This was the first reported compound that combined a high thermoelectric figure of merit with the pnp-switch.[6] However, the pnp-switching behavior has been observed only in nanocrystalline $AgBiSe_2$. If bulk material is used instead, the pnp-switch vanishes during the phase transition. In this case, only a pronounced dip in the Seebeck coefficient is found without a change of sign in the Seebeck values. Bulk-$AgBiSe_2$ is a n-type semiconductor[7,8] and turns into a p-type semiconductor upon partial substitution of Se by halides.[8]

Only two years later, in 2014, Biswas et al.[9] reported on pnp-switching in the mineral Stromeyerite AgCuS.[10] In this case, mobile silver ions cause a structural phase transition and induce a semi-metallic intermediate state during the transition that is responsible for the pnp-switch at 364 K. Electron transport is realized via the rigid sulfur sublattice while soft vibrations and mobility of Cu/Ag ions are responsible for effective phonon scattering and low thermal conductivity.

[a] *M. Sc. P. Deng, M. Sc. M. Hoffmann, Prof. Dr. T. Nilges*
Department of Chemistry, School of Natural Sciences (NAT)
Technical University of Munich (TUM)
Lichtenbergstraße 4, 85748 Garching b. München
E-mail: tom.nilges@tum.de

Guin and Biswas wrote an outstanding review on the pnp-switching materials known up to 2015.[4] They highlighted the principal concept and described the fundamental understanding of this process at that time. Although it has been stated by the authors that these compounds might have a potential application as diodes or transistors in the future, no experiments or methods were found in this direction up to that point.

In 2017, with $Tl_2Ag_{12}Se_7$, another pnp-switching compound was reported by Kleinke et al., which resulted from a systematic study on new thallium-based thermoelectric materials.[11] Due to its low total electrical conductivity and consequently low thermoelectric figure of merit > 0.035 at 578 K, this material is unfortunately not competitive in thermoelectric applications. Later on, it turned out that due to an artifact in the Seebeck measurements the postulated pnp-switch is not present in this material.[12]

Until last year, each reported pnp-switching compound showed this effect significantly above room temperature. For any application in IT technology or any other industry-relevant process, the switching temperature and the energy signature to reach and maintain this switch might be of crucial interest. In the following years since the discovery of $Ag_{10}Te_4Br_3$, the Nilges group tried to reduce the pnp-switching temperature towards room temperature. In 2023, such a room-temperature pnp-switching material was first reported after consecutive variations of the cation and anion substructures starting from $Ag_{10}Te_4Br_3$.[13] $Ag_{18}Cu_3Te_{11}Cl_3$ exhibits a pnp-switch at 290 K with a gigantic drop of the Seebeck coefficient of over 3000 $\mu V\,K^{-1}$ (at ≈ 295 K) followed by an increase of the thermopower by 4500 $\mu V\,K^{-1}$ (320 to 360 K). In contrast to all other materials denoted so far, $Ag_{18}Cu_3Te_{11}Cl_3$ is characterized by a 2-dimensional interaction of Te within a 3.6.3.6 Kagome-like layered arrangement that allows electron delocalization during the structural phase transition around room temperature. With the latter compound, an application of the pnp-switch to generate a position-independent and reversible diode at room temperature became reasonable, resulting in the first design of such a device with concrete evidence for the diode formation.[13] Slightly afterwards, AgCuS was used to construct a fast-switching diode at approximately 360 K where the orientation and reversibility of such a diode were illustrated. Especially, the alteration in the bias direction of the diode by reversing a temperature gradient has been proven for the first time in a semiconductor device.[14]

2. Materials with Pnp-Switching Properties

The following section briefly discusses the pnp-switching materials and their physical properties. The pnp-switch can be illustrated and identified by the Seebeck coefficient which changes its sign in a given temperature window. The Seebeck data of the pnp-switching materials discussed in this review are summarized in Figure 1.

In all cases, the switch is induced by a temperature change applied to the material. The main focus lies on the origin and mechanism of the pnp-switch. Furthermore, potential and already performed optimizations of this material class provide a valuable research area. Common characteristics of all materials constituting a pnp-switch are the following:

a) Incorporation of a mobile ionic species like Ag^+ or Cu^+, which allows ion transport in a solid.
b) Polymorphism with reversible phase transitions, driven by the cation (and sometimes also anion) mobility.
c) Semiconduction with a significant contribution of both ions and electrons to the conductivity.

Another important feature is the occurrence of covalency in certain subunits that allows the overlap of orbitals in such a way that electron delocalization can take place. In this case, a p-type or hole conduction is overcompensated or replaced by an electron conduction along these partially covalent-bonded subunits. This substructure can be either positively or negatively charged and is found in different cation and anion substructures of the materials. So far, only pnp-switching materials are

Prof. Dr. Tom Nilges has studied Chemistry at the University of Siegen since 1998. After his PhD at this University in 2001, he moved to the Universities of Regensburg and Münster to complete his Habilitation. In 2010 he became a professor of Inorganic Chemistry at the Technical University of Munich (TUM). His fields of interest are materials for energy conversion and storage, 2D and 1D materials based on group 15 elements, and hybrid solid ion conductors.

M. Sc. Philipp Deng is a third-year PhD student at the Technical University of Munich. After receiving his bachelor's (2018) and master's degree (2021) in Chemistry, he continued his research in the field of energy conversion materials. His current topic is focused on pnp-switchable coinage metal thermoelectrics and their utilization in fabricating single-material devices.
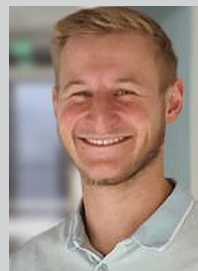
M. Sc. Matthias Hoffmann has received his B. Sc (2020) and M. Sc (2023) in chemistry from the Technical University of Munich. He is pursuing his PhD at the Technical University of Munich in the field of materials for energy conversion. His research topic focuses on the synthesis and characterization of new p–n-switchable polytellurides.
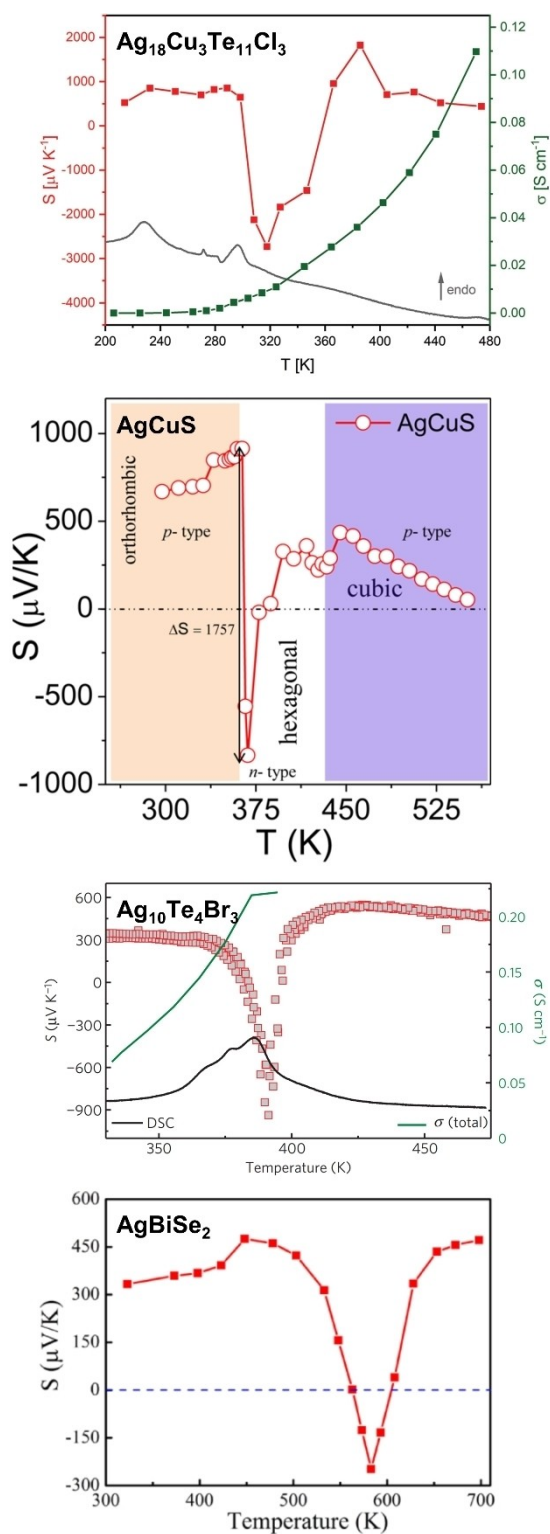
Figure 1. Seebeck measurements reported for pnp-switching materials. Original figures (pnp transition temperature) of $Ag_{18}Cu_3Te_{11}Cl_3$ (~290 K),[13] AgCuS (~364 K),[9] $Ag_{10}Te_4Br_3$ (~390 K),[5] and $AgBiSe_2$ (~560 K)[6] are reprinted with the permission of Wiley (Ref. 13, Copyright 2022), American Chemical Society (Ref. 6, Copyright 2012, Ref. 9, Copyright 2014) and Springer Nature (Ref. 5, Copyright 2009). Samples are presented according to their pnp-switching temperature from the lowest to the highest pnp-switching.

reported where the material is p-type semiconducting and the pnp-effect is caused by the nature of electronic interaction and induction of electron mobility, resulting in a temporary n-type behavior. No temporary p-type semiconduction or, more specifically, reversible generation of holes within a n-type semiconductor, and therefore, no thermally activated reversible npn-switch has been reported up to this point.

The discussion of the different material classes is presented in the order of their discovery instead of certain properties or aspects to show the progress in understanding the effect and the development of optimization strategies over time.

2.1. $Ag_{10}Te_4Br_3$ and Solid Solutions

$Ag_{10}Te_4Br_3$ has been synthesized in a solid-state melting and annealing process from Ag, Te and AgBr in stoichiometric amounts.[15,16] The structure can be described topologically by three different units concerning the anion substructure, a honeycomb or 6^3 Te^{2-} net, a 3.6.3.6 Br^- net and a linear polytelluride unit, that occur in a statistically disordered and also Peierls-distorted ordered arrangement (Figure 2).

This compound is a mixed electron and ion conductor that displays polymorphism with three reversible phase transitions in a temperature range from 290 to 360 K.[17] At first, the electric properties like the ionic conductivity (e.g. 7.5×10^{-4} S cm^{-1} at 301 K), which is approximately one order of magnitude lower than the electrical conductivity over the entire temperature range, and the complex structure chemistry including twinning and diffuse scattering phenomena were investigated. Due to the high ion mobility in the solid state, combined with the huge intrinsic defect concentration in the heavy-atom structure (Ag, Te), a determination of thermoelectric properties was initiated. It turned out that during the structural phase transition of β-$Ag_{10}Te_4Br_3$ starting at approximately 360 K, an intriguing and formerly unobserved pnp-switching effect occurred, depicted by a Seebeck drop of 1400 µV K^{-1} from $+310$ µV K^{-1} at 360 K to -940 µV K^{-1} at 390 K in the α-$Ag_{10}Te_4Br_3$ phase. During this phase transition which is characterized by a broad thermal signature of almost 50 K in Differential Scanning Calorimetry (DSC) measurements, the semiconductor type and therefore also the majority of charge carriers change from p-type (holes) to n-type (electrons). This previously undiscovered phenomenon cumulated to a more detailed study on the mechanism of this new physical effect and the development of an optimization strategy to maximize this property. At first, the mechanism of the pnp-switch was examined in detail.[5] A combination of electrochemical measurements, temperature-dependent Solid-State NMR spectroscopic investigations in the Ag and Te substructures, and brief quantum-chemical modeling of the Te substructure illustrated that a Peierls distortion phenomenon in the polytelluride substructure, in combination with the mobile Ag ion substructure, is the origin of the change of majority charge carriers from holes to electrons during the structural phase transition. $Ag_{10}Te_4Br_3$ is a p-type semiconductor at most temperatures which is overlaid by a n-type conduction along a linear chain of
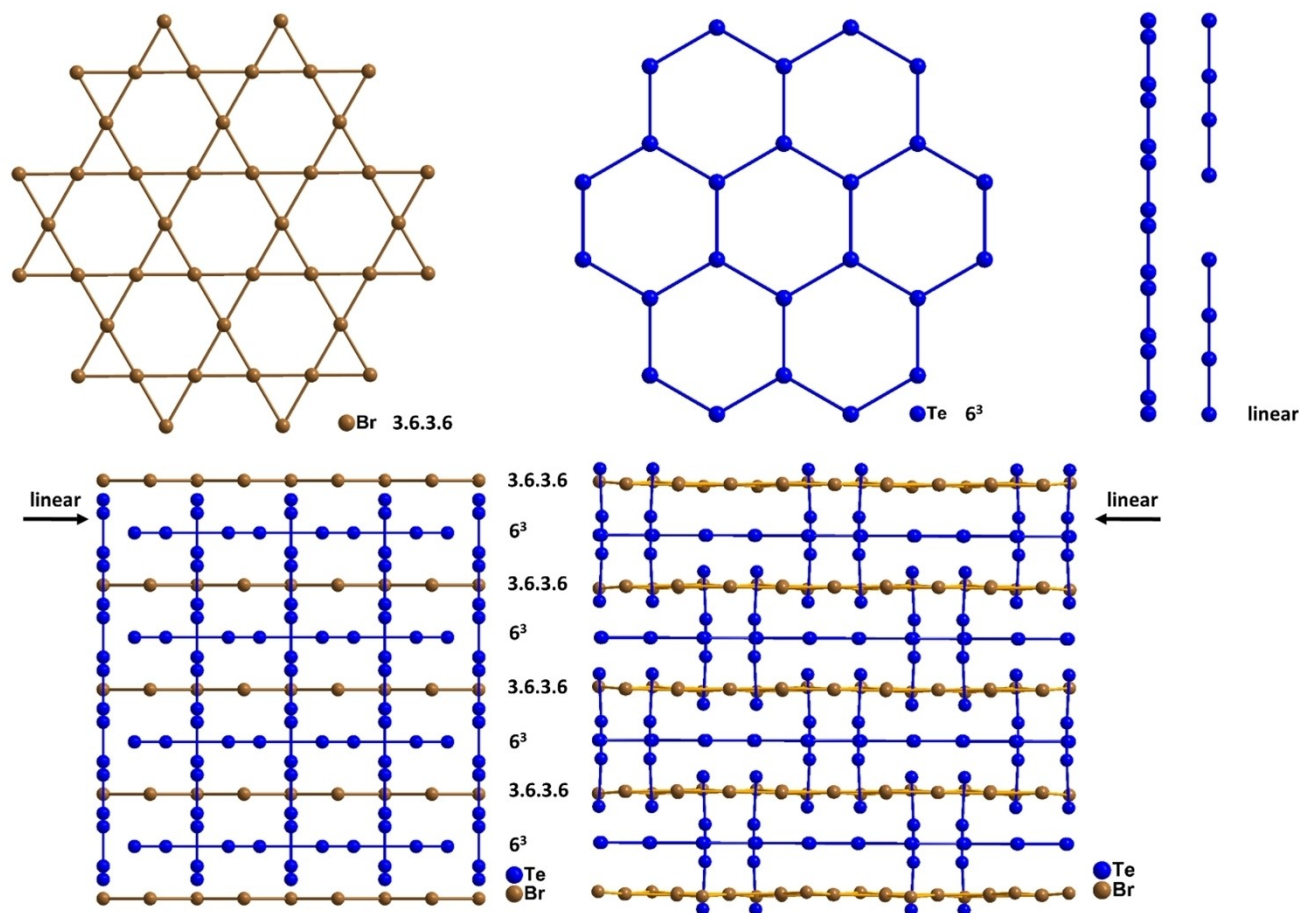
Figure 2. Top row: Structure building units in the anion substructure of $Ag_{10}Te_4Br_3$. A 3.6.3.6 Br, 6^3 Te, and a linearly-arranged $[Te_4]$ unit are present in $Ag_{10}Te_4Br_3$. Bottom row: Arrangement of the anion units in α-$Ag_{10}Te_4Br_3$ at 410 K and γ-$Ag_{10}Te_4Br_3$ at 223 K.[17]

partially covalent bonded telluride. Via Electron Localization Function (ELF) and band structure calculations it could be illustrated that such an electron delocalization takes place in this subunit. Solid State Te-NMR spectroscopy around the 360 K phase transition substantiated this finding via a coalescence phenomenon that occurred when the Peierls-distorted, static state in the polytelluride substructure (covalent $[Te_2]^{2-}$ dumb-bells and isolated Te^{2-} ions) disappeared and resulted in an intermediate equidistant Te chain after the dynamic reorientation of Te. Upon further mobility increase in the linear unit this linear chain transforms to a double maxima situation as stated in Figure 2. This equidistant and partially covalently-bonded Te chain allows electron transport along the structure due to a significant orbital overlap. Precisely this dynamic reorientation of the linear polytelluride substructure is mandatory for the pnp-switch.

After the identification of the origin of the pnp-switch, a systematic study of solid solutions was initiated to examine the influence of partial substitution in the coinage metal, chalcogenide and halide substructure on the pnp-switch. A substitution is possible in all three different substructures of $Ag_{10}Te_4Br_3$, as

Ag can be partially replaced by Cu, Te by Se and S, and Br by Cl and I. Especially the substitution within the chalcogenide substructure is of high interest because the origin of the pnp-switch is located within the linear polytelluride substructure. As expected, the substitution of Te by the lighter or heavier homolog resulted in a significant impact on the Seebeck coefficient.[18] The absolute value of the Seebeck drop is strongly dependent on this substitution and even small substitution grades of 5 to 10% in $Ag_{10}Te_{3.8}S_{0.2}Br$ or $Ag_{10}Te_{3.9}Se_{0.1}Br_3$ caused a drastic reduction of the Seebeck drop and a loss of the pnp-switch. Due to the statistical distribution of the chalcogenide in the anion substructure, the linear polychalcogenide chain is not able to perform the necessary chain dynamic anymore and only non-substituted chains are capable of initiating the electron delocalization and pnp-switch. Interestingly, the substitution within the halide substructure positively affects the magnitude of the Seebeck drop and therefore the pnp-switch. Partial halide substitution of Br by Cl up to x=1.2 in $Ag_{10}Te_4Br_{3-x}Cl_x$ resulted in the biggest Seebeck drop of 1800 $\mu V K^{-1}$ in $Ag_{10}Te_4Br_{2.6}Cl_{0.4}$,[18] but also slightly increased the pnp-phase transition temperature by 11 K.[19] Iodide substitution, on the other, hand reduces

the phase transition temperature[20] and the Seebeck drop.[18] While the halide substructure is not directly involved in the pnp switch, it determines and accomodates the polytelluride subunit. The substitution, depending on the replacing halide, increases or decreases the available space for the polytelluride subunit in these solid solutions, which has an impact on the Seebeck drop and the phase transition temperature. Another aspect of the halide substructure in this materials class is that it acts as a quasi-cation barrier within the structure. The Ag^+ cations seem to be unable to move through the 6^3 halide nets.

A positive side effect of the substitution study was that many other coinage metal polychalcogenide halides such as $Ag_{23}Te_{12}X$ (with X=Cl, Br),[21] $Ag_{19}Te_6Br_7$,[20] $Ag_{1.54}Te$,[22] $Cu_{9.1}Te_4Cl_3$,[23] and $Cu_{20}Te_{11}Cl_3$,[24] with comparable subunits but different structural arrangements were discovered. The interested reader is asked to follow this aspect in recent literature.[25] Later on, it was reported that many of the discussed coinage metal polychalcogenides are variants of minerals that can be found in nature.[26] At that time, when $Ag_{10}Te_4Br_3$ and related compounds were discovered, the search for additional pnp-switching compounds was initiated. The following subchapters illustrate the recent findings of other known pnp-switching classes of materials that have been discovered in the past 15 years.

2.2. AgBiSe₂ and Related Materials

$AgBiSe_2$ is a prominent semiconductor,[27] thermoelectric[28] and solar cell material[29] which gathered high interest even before and after the discovery of the pnp-switching effect.

In their article, Yang, Xie and coworkers reported a thermoelectric figure of merit ZT of 1.5 for nano-crystalline $AgBiSe_2$ at 700 K which qualifies $AgBiSe_2$ as a reasonable thermoelectric material.[6] The thermoelectric characterization also revealed, that nanocrystalline $AgBiSe_2$, which undergoes two reversible phase transitions at ~410 K and ~580 K (see Figure 3), shows a pnp-switch at the high-temperature transition where rhombo-hedral $AgBiSe_2$ transforms to disordered rock salt-like $AgBiSe_2$.[6] The Seebeck coefficient varies between $480\,\mu V K^{-1}$ and $-250\,\mu V K^{-1}$ in a broad temperature range starting approximately 80 K below the phase transition. The electronic and also pnp-switching properties differentiate drastically if nano-crystalline material prepared by solution-based methods is compared to larger-sized bulk particles obtained via a classical solid-state annealing route. Micrometer-sized or bulk-$AgBiSe_2$ is, in contrast to the confined nano-sized material, a n-type semiconductor.[7] Substitution experiments demonstrate that Bi can be replaced partially by Pb and Ag by Nb to a certain degree. In the $AgBi_{1-x}Pb_xSe_2$ system which is still n-type for x=0 to 0.02, further Pb content increase leads to p-type conduction for x=0.025 to 0.06. This behavior is explained by a simple electron count calculation. Starting from pristine n-type $AgBiSe_2$, Pb^{2+} doping on Bi^{3+} sites first results in a decrease in the electron concentration up to the point when the Pb^{2+} concentration exceeds the intrinsic electron concentration. At this point, the compound switches to p-type conduction.[7] Using Nb-substitution on the Ag site in $Ag_{1-x}Nb_xBiSe_2$, which represents an electron doping process, resulted in n-type conductors for all substitution rates of x=0.02 to 0.04. At the high-temperature phase transition, where in nano-particular $AgBiSe_2$ the pnp-switch occurred, a pronounced Seebeck anomaly towards higher (more negative) Seebeck values was observed. This effect was attributed to a Charge Density Wave (CDW) within the Ag–Bi cation sublattice that causes this Seebeck anomaly. Upon increase of the Nb content, the Ag–Bi substructure and therefore the CDW interaction has partially been hindered by an increasing Nb content. As a result, the irregularity is reduced by a higher Nb content.

Later on, halide substitution was performed in $AgBiSe_{2-x}X_x$ with X=Cl, Br, I, and x=0.02, 0.04.[8] All materials show n-type semiconduction over the entire temperature range and also a halide-independent anomaly of the Seebeck coefficient similar to the previous Nb-substituted phases. Since the Ag–Bi substructure is not affected by halide substitution in the anion substructure, this finding is consistent with the previous interpretation of the anomaly.
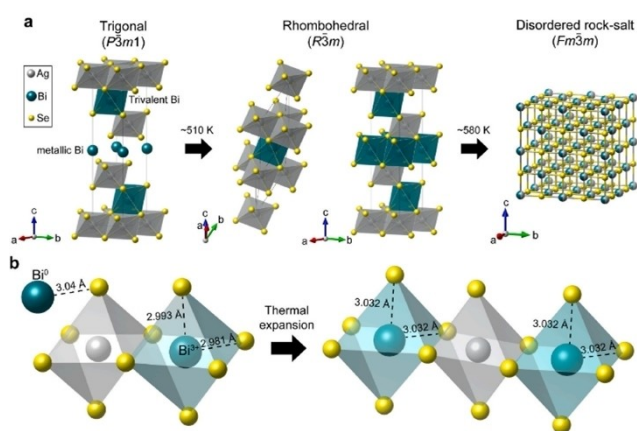
2.3. AgCuS, a Mineral

The previous material suggests, that nanoconfinement and particle size could be critical requirements for the pnp-switching behavior. However, this subchapter illustrates that other material properties are more likely to be responsible for the pnp-switch and nano-sized particles are even detrimental in some cases.

$AgCuS$ is a mineral called Stromeyerite[10] that has gained reasonable interest due to its high ion mobility and polymorphism (Figure 4). It was first described by Strohmeyer in 1816 and subsequently identified as a 1:1 ($Cu_2S:Ag_2S$) compound accessible from the binary sulfides.[30] Later investigation revealed that the mineral shows a certain silver deficit and can be described as $Ag_{1-x}CuS$ with x=0 to 0.1 to be more precise.[31] For simplicity, we continue to use the term AgCuS in the

Figure 3. Crystal structures of $AgBiSe_2$ polymorphs. Reprinted from Ref. 28, with permission from Elsevier, copyright 2023.
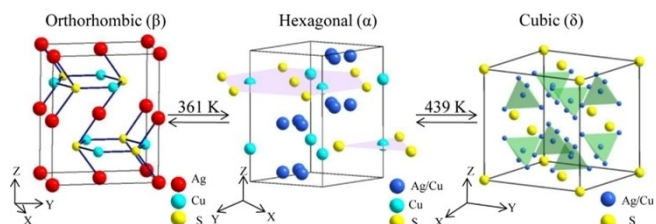
Figure 4. Crystal structures of AgCuS polymorphs. Reprinted with permission from Ref. 9. Copyright 2014 American Chemical Society. The low temperature γ-phase, space group $Pmc2_1$ is missing in this figure.[10]

manuscript, in accordance with the literature. At ambient pressure, AgCuS is characterized by three reversible phase transitions at 120 K, 361 K and 439 K.[10] For our purpose, the interesting pnp-transition is the one at 361 K where β-AgCuS transforms to α-AgCuS. A sharp drop of the Seebeck coefficient from a peak of 917 $\mu V K^{-1}$ at 364 K to $-840\ \mu V K^{-1}$ within a temperature range of 3 K is observed.

During this transition, the silver substructure tends to become disordered while the copper one stays ordered (Figure 4). Together with the aforementioned slight disorder in the silver substructure, this behavior is expected. Both high-temperature phases, the α- and δ-phase are solid ion conductors which is consistent with the degree of disorder in the cation substructure. In an excellent combination of quantum chemical calculations, positron annihilation spectroscopy and Raman spectroscopy Biswas et al. were able to determine the origin of the pnp-switch during the β–α phase transition, where in an intermediate structure stage between the orthorhombic and hexagonal phase the states near Fermi energy are dominated by sulfur orbitals. Electron conduction is realized via the covalently bonded Cu–S substructure, as it was identified that a contribution from hybridized Cu–S orbitals to the overlapping valence and conduction band gives rise to a semi-metallic character. As a consequence electron delocalization can take place and n-type conduction results. This interaction is two-dimensional, in contrast to the previously discussed compounds that show a one-dimensional interaction for electron transport. All observations were made on bulk material that was prepared by a solid-state melting and annealing process.[9]

When AgCuS is synthesized as nano-crystalline material using a more kinetically controlled, liquid-based, wet-chemical approach the situation changes profoundly.[32] Biswas and coworkers performed a size-dependent analysis of the pnp-switching property with agglomerated nano-sized particles of ~40 nm and ~120 nm average diameters. It turned out that the pnp-switch vanishes for these nano-sized particles and only a drop in the positive Seebeck values occurrs from 783 $\mu V K^{-1}$ to 418 $\mu V K^{-1}$ (see Figure 5). With increasing size of the particles the drop becomes larger and tends to move towards the bulk properties.

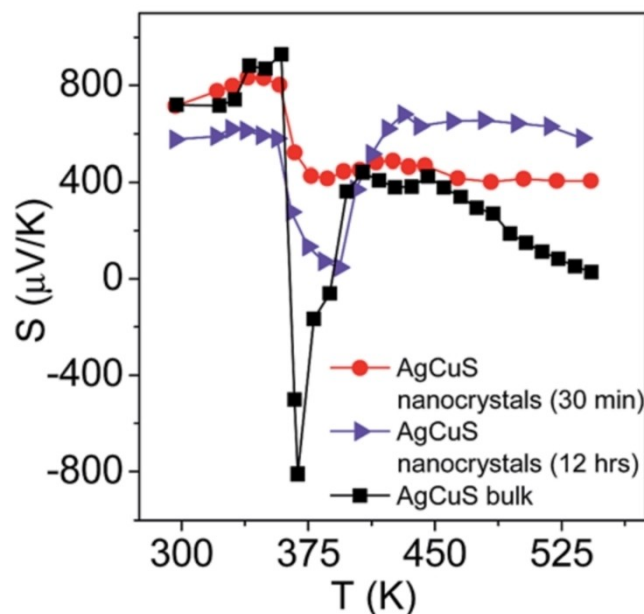40 nm nano-sized AuCuS show a higher band gap of 1.2 eV compared to the 0.9 eV for the bulk phase, whereas the charge

Figure 5. Seebeck measurements of AgCuS nanocrystals of ~40 nm (30 min), ~120 nm average diameters (12 hrs) and bulk material. Reproduced from Ref. 32 with permission from the Royal Society of Chemistry.

carrier concentration and conductivity are higher for the nano-sized material at 300 K. Biswas et al. reported that the band gap increase is the primary reason for the vanishing pnp-transition (Figure 5).

2.4. $Tl_2Ag_{12}Se_7$

In 2017, Kleinke et al. reported on a reversible pnp-switch in $Tl_2Ag_{12-x}Se_7$ where the Seebeck coefficient changed from $+230\ \mu V K^{-1}$ at 390 K to $-230\ \mu V K^{-1}$ at 410 K, and then back up to $+75\ \mu V K^{-1}$ at 420 K.[11] A hypothesis for the origin of this effect by the authors was the disorder of Se within a linear arrangement in the anion substructure. Se showed enlarged displacement parameters along the chain direction which was interpreted as a disorder phenomenon like in the partially covalent bonded substructure in $Ag_{10}Te_4Br_3$. It has been stated in the manuscript that an analogous disorder phenomenon in a structurally closely related $Tl_4Ag_{24-x}Te_{15-y}$ phase[33] where a Te chain shows a comparable disorder did not lead to a pnp-switch. After a more detailed investigation of the materials and the measurements by the authors it turned out that the pnp-switch was caused by an artifact in the Seebeck measurements due to an erroneously recorded slope of the Seebeck coefficient.[12] A X-ray Photoelectron Spectroscopy investigation during the structural phase transition at the point where the pnp-switch was supposed to occur did not show any change in the electronic states of any element in the compound. Therefore, this compound will not be discussed any further in this review.

2.5. $Ag_{18}Cu_3Te_{11}Cl_3$: Pnp-Switching at Room Temperature

Since $Ag_{10}Te_4Br_3$ has been discovered, one idea was to reduce the pnp-switching temperature from elevated temperatures (see Table 1) to room temperature to get this effect in a more applicable temperature region.

A fundamental approach in materials science to achieve such a goal is to maintain the important substructures or units in such a material that are responsible for a certain physical effect and modify the remaining structure to reach that goal. This has been performed for $Ag_{10}Te_4Br_3$ in the past 13 years. As already stated in chapter 2.1 a plethora of new coinage metal chalcogenide halides were discovered during this optimization process. Following the general synthesis recipe for the realization of a pnp-switching material, that includes the utilization of mobile ions (d^{10} ions), a partially covalently bonded substructure (chalcogenide), being capable of performing electron delocalization, and an innocent but structure-directing halide substructure, finally resulted in the discovery of $Ag_{18}Cu_3Te_{11}Cl_3$.

It shows two reversible phase transitions at 218(3) K from γ-$Ag_{18}Cu_3Te_{11}Cl_3$ to β-$Ag_{18}Cu_3Te_{11}Cl_3$. and at 288(3) K to α-$Ag_{18}Cu_3Te_{11}Cl_3$. During the β−α phase transition, a pnp-switch with an extraordinarily huge Seebeck drop of 4500 $\mu V K^{-1}$ occurs right after the structural phase transition.

The material is structurally related to $Ag_{10}Te_4Br_3$ due to similar building blocks that occur in both compounds (Figure 6). Using a simple topologic approach to describe the crystal structure, common building blocks or subunits present in both compounds are a 3.6.3.6 Kagomé net (Cl, Br and Te), a 6^3 honeycomb net (Te), and a linear unit (Te). The Te 3.6.3.6 net is distorted (see Figure 6).

In $Ag_{10}Te_4Br_3$, an alternating stacking of a 3.6.3.6 Br Kagomé and a 6^3 Te net is realized where the linear Te unit is accommodated perpendicular to the nets in suitable channels. The Peirls-distortion within the Te chain below the pnp-switching temperature is modulated towards an equidistant chain during the pnp-switch. Alternating Kagomé and honeycomb nets are also present in $Ag_{18}Cu_3Te_{11}Cl_3$ but here every second halide Kagomé net is replaced by a distorted Te net. This exchange leads to a slightly modified composition compared with $Ag_{10}Te_4Br_3$. First Br is fully replaced by Cl and the Te substructure was modified to allow a higher chalcogenide content. Taking the anion substructure $[Te_4X_3]$ (with X = halide) and multiplying it by two leads to $[Te_8X_6]$. Replacement of half of the X by Te resulted in $[Te_{11}X_3]$ for the anion substructure in $Ag_{18}Cu_3Te_{11}Cl_3$. While the formal charge of Cl is −1, the Te charge is defined by the bonding situation of the chalcogen atoms on the different sites. The 6^3 net consists of isolated Te^{2-} ions while the distorted 3.6.3.6 Te net and the linearly Te chain are composed of $[Te_2]^{2-}$ and isolated Te^{2-} ions. A full replacement of Ag by Cu resulted in $Cu_{20}Te_{11}Cl_3$[24] which did not show a pnp-switch. Neither the linear Te nor the Te 3.6.3.6 substructure showed a suitable bonding or disorder phenomena to allow effective electron transport. The linear Te subunit in $Cu_{20}Te_{11}Cl_3$ is characterized by slightly elongated $[Te_2]^{2-}$ dumbbells not capable of performing a Peierls distortion (refer to Figure S1, Supplement) and the 3.6.3.6 Te Kagomé net is orientationally disordered in all polymorphs over the entire temperature range up to the decomposition point of the material.

A significant portion of Cu needed to be replaced by Ag to initiate pnp-switching. This effect is related to an increase in the cell volume and the modification of the linear Te subunit towards an ordered $[Te_4]$ unit as observed in $Ag_{10}Te_4Br_3$ (see Figure 6). As a consequence of the cell enlargement and Ag incorporation the 3.6.3.6 Te Kagomé net now shows a dynamic rearrangement and ordering during the pnp-switching phase transition. In a combined temperature-dependent single crystal structure and Solid-State NMR spectroscopic analysis of $Ag_{18}Cu_3Te_{11}Cl_3$ the origin and mechanism of the pnp-switch between 295 and 360 K, right after the structural phase transition of 288 K, was determined and analyzed. Two different origins of the switch were identified, a dynamic interaction of

Table 1. List of pnp-switching compounds with pnp-switching temperature and Seebeck coefficient range.

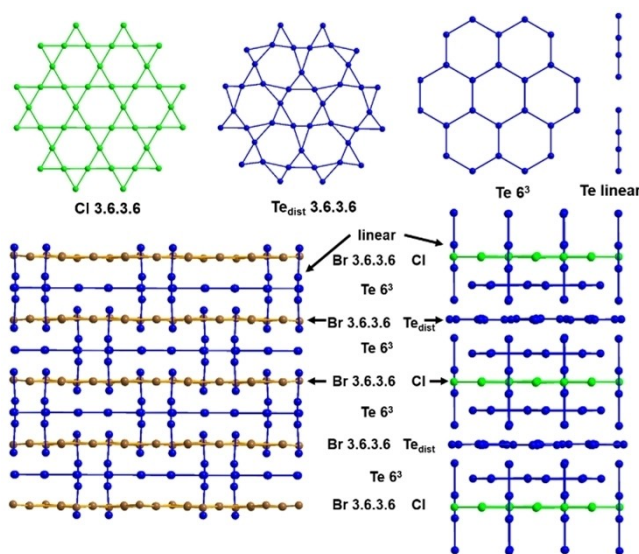| Compound	pnp-switch temperature/K	Seebeck coefficients (drop)/ $\mu V K^{-1}$	Literature
$Ag_{10}Te_4Br_3$	390	+540 to −940 (1480)	[5]
$Ag_{10}Te_4Br_{2.6}Cl_{0.4}$	387	+500 to −1300 (1800)	[18]; [34]
$AgBiSe_2$	560	+480 to −250 (730)	[6]
$AgCuS$	364	+917 to −840 (1757) +648 to −393 (1041)	[9] [14]
$Ag_{18}Cu_3Te_{11}Cl_3$	295	1800 to −2700 (4500)	[13]

Figure 6. Similarities and differences of the crystal structures of $Ag_{10}Te_4Br_3$ (bottom left) and $Ag_{18}Cu_3Te_{11}Cl_3$ (bottom right).

Te in the 3.6.3.6 Te Kagomé net and a d^{10}–d^{10} interaction in the coinage metal cation substructure. are responsible for this intriguing effect. The cations show different mobilities upon temperature increase while Cu^+ is significantly less mobile than Ag^+. The interplay of the mobile cations and the covalence in bonding within the 3.6.3.6 Te Kagomé net drives the pnp-switch and is also responsible for the magnitude of the Seebeck drop.

Previously mentioned materials show changes during the pnp-switch of only 1480 μVK^{-1} in $Ag_{10}Te_4Br_3$, 730 μVK^{-1} in $AgBiSe_2$, and 1757 μVK^{-1} in AgCuS, whereas $Ag_{18}Cu_3Te_{11}Cl_3$ is characterized by a Seebeck change of more than 4500 μVK^{-1} during the switch from n-type back to p-type semiconduction above 320 K. This 4500 μV drop represents the highest reported Seebeck drop for any pnp-switching material so far.

N–p transitions are sometimes observed for low-Seebeck materials. One example is $Cs_8Cd_{18}Sb_{28}$ where a n-p transition occurs at temperatures below 100 K.[35] The origin of such n-p transition is often different from the one discussed in this review.

3. Application of Pnp-Switching Materials in Devices

For many years the pnp-switching materials were curiosities with interesting physical properties like low thermal conductivity, high ion mobility and polymorphism, but a direct application was not reported. This is somewhat unusual because semiconductors are important materials in many electronic applications, energy conversion processes and catalysis. In this chapter, we summarize the utilization of $Ag_{18}Cu_3Te_{11}Cl_3$ and AgCuS as the first materials to generate reversible, position-independent one-compound pn-junctions and diodes. A so-called one-compound diode is a paradigm change for the generation and utilization of diodes. The complex process of doping itsef and applying a p- and n-type semiconductor on fixed positions on devices may be replaced by deposition of a single material. This material can then be manipulated accordingly to generate a diode or potentially even a transistor by a temperature pulse when needed, which is temporary and can be deleted right after its utilization. A more flexible and position-independent usage of diodes and transistors in devices is probable and the choice of the rectifying direction dependent on the applied T-gradient might be of interest. These features are impossible to realize once an Integrated Circuit (IC) is generated using state-of-the-art technology. Future prospects are the miniaturization of diode devcices and the materials towards the nano regime where the temperature gradient might be induced by lasers and the incorporation of magnetic properties, via substitution of the cations, i.e. 2 Cu^+ by Mn^{2+}.

3.1. The First Room-Temperature One-Compound Diode $Ag_{18}Cu_3Te_{11}Cl_3$

As $AgBiSe_2$ and $Ag_{10}Te_4Br_3$ exhibit pnp-switches that are too far away from a suitable and economic operation temperature for most processes, the first materials to be assessed as potential one-compound diodes were the ones with the switch closest to the room temperature, $Ag_{18}Cu_3Te_{11}Cl_3$ and AgCuS.

A device was constructed using a custom designed printed circuit board with $Ag_{18}Cu_3Te_{11}Cl_3$ soldered on it and miniature surface mount resistors on one side to provide temperature control via addressable, nonuniform resistive heating. It was the first material where a diode behavior with a forward current over 10 times larger than the reverse current at ±1.0 V was observed. A junction potential of 0.3 V was determined for $Ag_{18}Cu_3Te_{11}Cl_3$ being held in a temperature gradient of 295 to 308 K. Following the structural and electronic features during the diode formation a new type of junction, an ambijunction, was defined to describe the ambivalent character of the new diode type.

The constructed device using $Ag_{18}Cu_3Te_{11}Cl_3$ behaves ohmically when it is kept isothermally at any temperature within and out of the pnp-switching phase transition without any diode characteristics. An example is illustrated in Figure 7 at 281 K where $Ag_{18}Cu_3Te_{11}Cl_3$ is firmly stable in the β-phase.

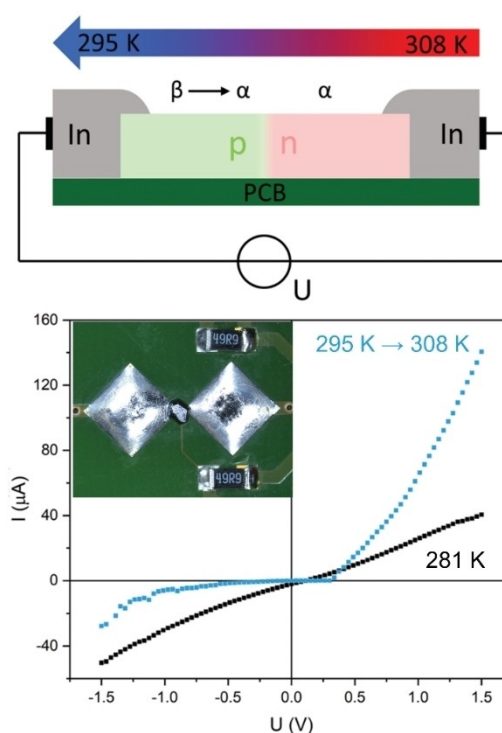**Figure 7.** Top: Schematic illustration of $Ag_{18}Cu_3Te_{11}Cl_3$ mounted on a Printed circuit Board (PCB) with p- and n-type regions generated by a temperature gradient. Bottom: I–U curves of $Ag_{18}Cu_3Te_{11}Cl_3$ treated isothermally at 281 K and within a temperature gradient of 295 to 308 K. Inset: PCB with mounted $Ag_{18}Cu_3Te_{11}Cl_3$ crystal and resistors for resistivity headting. Reprinted with permission from Ref. 13. Copyright 2022 Wiley.

The switching time for the removal of the excess charge carriers in polarization experiments (± 5 V window) was 8.7 s and the fall time to reach 10% of the initial reverse current was 62.4 s (Table 2).

As previously mentioned, the temperature-dependent mechanism behind this effect was evaluated by a combined thermoanalytic, diffraction and spectroscopic approach. In Differential Scanning Calorimetry (DSC) measurements combined with temperature-dependent X-ray diffraction studies it became clear that after a structural phase transition at 290 K a reversible and continuous rearrangement in the 3.6.3.6 Te Kagomé net occurred which can be regarded as a dynamic 2D charge density wave capable to delocalize electrons across the net (Figure 8). Another aspect driving the pnp-switch is the occurrence of d^{10}–d^{10} interactions within the coinage metal cation substructure. The d^{10} ion distances within the cation substructure becomes smaller upon heating within the n-type region between 290 and 320 K.

This attractive d^{10}–d^{10} interaction in combination with the charge density wave is responsible for effective electron delocalization and mobility in $Ag_{18}Cu_3Te_{11}Cl_3$. A comparable increase in attractive interactions was stated by Biswas et al. for AuCuS where a strong covalency in the planar framework of Cu and S is responsible for electron conduction.[9]

Table 2. Characteristics and thermal conditions of pnp-switching compounds used as diodes in devices.

Compound	T-gradient/K	Switching time t_s/s	Fall time t_f/s	Literature
AgCuS	333–368	2.5	$\ll 10^{-3}$	[14]
$Ag_{18}Cu_3Te_{11}Cl_3$	295–308	8.7	62.4	[13]
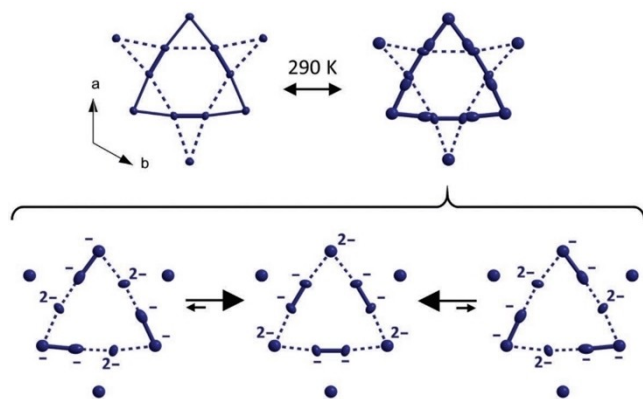
Figure 8. Structure section of the 3-6-3-6 Te net in $Ag_{18}Cu_3Te_{11}Cl_3$ right after the 288 K β-$Ag_{18}Cu_3Te_{11}Cl_3$. to α-$Ag_{18}Cu_3Te_{11}Cl_3$ phase transition. The mechanism of $[Te_2]^{2-}$-dumbbell delocalization within the 3.6.3.6 Te Kagomé section is illustrated. The most important mesomeric form is still the one in the middle where the $[Te_2]^{2-}$-dumbbell is centered in the Te triangle. The population of the additional Te position leads to a rearrangement of the dumbbell. Reprinted with permission from Ref. 13. Copyright 2022 Wiley.

3.2. AgCuS, a One-Compound Diode with Fast Switching Speed

Based on the successful realization of a one-compound diode with $Ag_{18}Cu_3Te_{11}Cl_3$, AgCuS was the second compound tested with a similar setup.[14] In contrast to the previous one the pnp-switch occurs at slightly higher temperatures of approximately 364 K. The diode was successfully formed using a temperature gradient of 333 to 368 K with p-type conduction present on one side at 333 K whilst AgCuS is in its n-type stage on the other side at 368 K. The significantly bigger single crystals of this material allowed for a broader temperature range across the crystal, therefore enabling a more extensive temperature-dependent study of the current-voltage characteristics during the pn-junction formation, which also encompassed the heating and cooling processes before and after reaching the temperature gradient, respectively. The switching time is reduced slightly to 2.5 s while the fall time is reduced tremendously below 10^{-3} s.

Aside from these basic diode characteristics, the reversibility of diode formation and the flexibility of current flow direction were illustrated for the first time for a one-compound diode. In consecutive experiments the temperature gradient was switched on and off changing the I/U characteristics from pure ohmic at 298 K to the diode characteristics within a 333 to 368 K temperature gradient (see Figure 9, top part). In common diode devices, as used in IT technology, the direction of the current flow and the bias direction are defined by the position of the p- and n-regions. If the semiconductor type can be selected dependent only on temperature, as in the title compounds, one can gain another level of flexibility concerning the application of the diode. As shown in the bottom part of Figure 9, the diode's forward direction is correlated with the applied temperature gradient and can be changed to the opposing direction by flipping the temperature gradient. As proven by the shape of the I–V curve under isothermal and non-isothermal conditions the direction of the pn-junction located in AgCuS can be reversed.

4. Conclusions

Since the discovery of the first pnp-switching compound, $Ag_{10}Te_4Br_3$, three additional systems were reported that show this intriguing effect. All compounds are characterized by reversible structural phase transitions that are driven by mobile coinage metal cations. A second prerequisite is the occurrence of attractive bonding interactions or covalency in structure subunits which is necessary to allow effective electron delocalization and transport. This generation of covalency can be regarded as an overlaying metal-like electron-conducting state within a hole-conducting system. In some cases, a band-gap closure was found during the p- to n-transition being responsible for the electron conduction which disappeared again upon further temperature increase. Important for such an electronic effect is a CDW within a certain substructure, including the reversible rearrangement of atoms that allows the
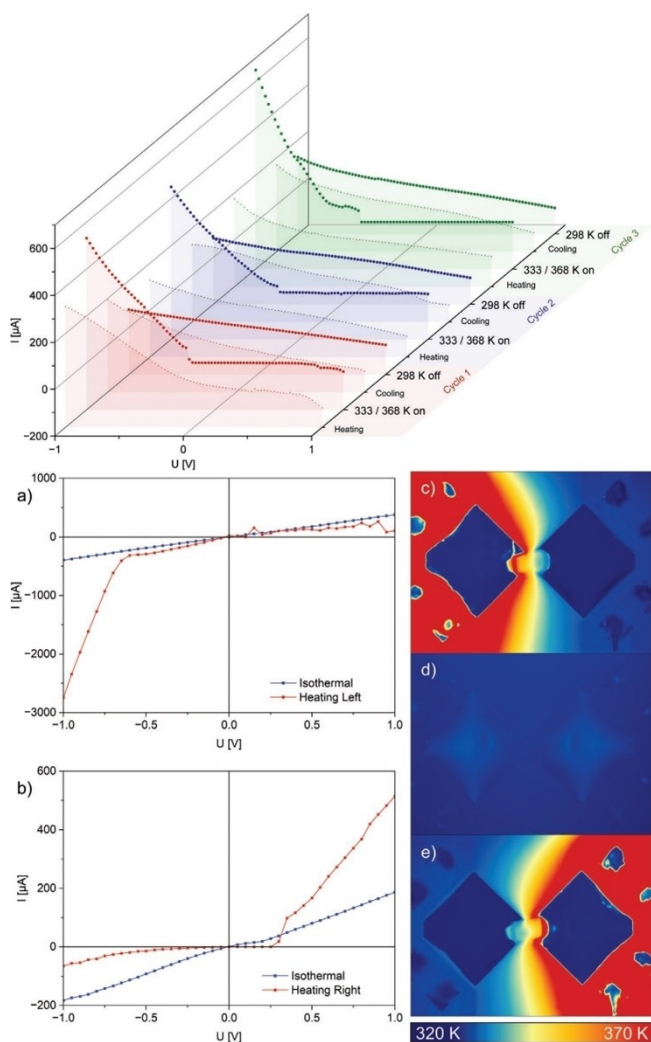
Figure 9. Top part: Reversible switching between a simple ohmic p-type semiconduction in AgCuS at 298 K and the pn-diode within a 333 to 368 K temperature gradient. Bottom part: Current flow reverse upon temperature gradient flip in AgCuS. I/U measurements and an IR camera picture illustrating the applied temperature gradient are shown. Reprinted with permission from Ref. 14. Copyright 2023 Wiley.

certain impact on catalysis and related processes where such a reversible and addressable adjustment of opposite charge carriers are of interest.

Acknowledgements

Conflict of Interest

The authors declare no conflict of interest.

fluctuation of electrons. While the discovery of new pnp-switching compounds dominated the research in the beginning, the objective shifted towards potential applications of these materials recently. Due to the fact that after more than 15 years since the discovery of the first pnp-switching material only a handful of compound are known which are capable to reversibly switch its semiconductor properties, machine learning might be utilized to find more of these intriguing materials and computational chemistry is a powerful tool to predict new phases. For two of the four known materials diode devices were successfully fabricated and tested. $Ag_{18}Cu_3Te_{11}Cl_3$ is capable of being used as a volatile, position-independent diode at room temperature that offers opportunities for new IT architectures and multifunctional devices. The generation, control and local positioning of holes and electrons charge carriers might have a

[1] Water splitting and photocatalysis: a) T. Hisatomi, J. Kubota, K. Domen, *Chem. Soc. Rev.* **2014**, *43*, 7520–7535; b) F. Zhang, X. Wang, H. Liu, C. Liu, Y. Wan, Y. Long, Z. Cai, *Appl. Sci.* **2019**, *9*, 2489; c) J. S. Lee, *Catal. Surv. Asia* **2005**, *9*, 217–227.
[2] Pn diodes and transistors: a) T. J. Flack, B. N. Pushpakaran, S. B. Bayne, *J. Electron. Mater.* **2016**, *45*, 2673–2682; b) Y. Pan, B. Yang, *Highlights in Science, Engineering and Technology* **2024**, *87*, 214–218.
[3] Doping/ Deposition: a) K. Rajeshwar, *Encycl. Electrochem.* **2007**, *6*, 1–53; b) W. Stutius, *J. Cryst. Growth* **1982**, *59*, 1–9.
[4] Physical properties and effects: a) S. N. Guin, K. Biswas, *Phys. Chem. Chem. Phys.* **2015**, *17*, 10316–10325; b) J. Mannhart, A. Kleinsasser, J. Ströbel, A. Baratoff, *Physica C* **1993**, *216*, 401–416; c) J. Liu, T. Gottschall, K. P. Skokov, J. D. Moore, O. Gutfleisch, *Nat. Mater.* **2012**, *11*, 620–626; d) N. Rangaraju, P. Li, B. W. Wessels, *Phys. Rev. B* **2009**, *79*, 205209.
[5] T. Nilges, S. Lange, M. Bawohl, J. M. Deckwart, H.-D. Wiemhöfer, R. Decourt, B. Chevalier, J. Vannahme, H. Eckert, R. Weihrich, *Nat. Mater.* **2009**, *8*, 101–108.
[6] C. Xiao, X. Qin, J. Zhang, R. An, J. Xu, K. Li, B. Cao, J. Yang, B. Ye, Y. Xie, *J. Am. Chem. Soc.* **2012**, *134*, 18460–18466.
[7] L. Pan, D. Bérardan, N. Dragoe, *J. Am. Chem. Soc.* **2013**, *135*, 4914–4917.
[8] S. N. Guin, V. Srihari, K. Biswas, *J. Mater. Chem. A* **2015**, *3*, 648–655.
[9] S. N. Guin, J. Pan, A. Bhowmik, D. Sanyal, U. V. Waghmare, K. Biswas, *J. Am. Chem. Soc.* **2014**, *136*, 12712–12720.
[10] D. Santamaria-Perez, A. Morales-Garcia, D. Martinez-Garcia, B. Garcia-Domene, C. Muhle, M. Jansen, *Inorg. Chem.* **2013**, *52*, 355–361.
[11] Y. Shi, A. Assoud, C. R. Sankar, H. Kleinke, *Chem. Mater.* **2017**, *29*, 9565–9571.
[12] Y. Shi, *Ph.D. Thesis*, Univ. Waterloo **2020**.
[13] A. Vogel, A. Rabenbauer, P. Deng, R. Steib, T. Böger, W. G. Zeier, R. Siegel, J. Senker, D. Daisenberger, K. Nisi, *Adv. Mater.* **2023**, *35*, 2208698.
[14] P. Deng, A. Rabenbauer, K. Vosseler, J. Venturini, T. Nilges, *Adv. Funct. Mater.* **2023**, *33*, 2214882.
[15] S. Lange, T. Nilges, *Chem. Mater.* **2006**, *18*, 2538–2544.
[16] T. Nilges, M. Bawohl, S. Lange, *Z. Anorg. Allg. Chem.* **2006**, *632*, 2088.

[17] S. Lange, M. Bawohl, D. Wilmer, H.-W. Meyer, H.-D. Wiemhöfer, T. Nilges, *Chem. Mater.* **2007**, *19*, 1401–1410.

[18] O. Osters, M. Bawohl, J.-L. Bobet, B. Chevalier, R. Decourt, T. Nilges, *Solid State Sci.* **2011**, *13*, 944–947.

[19] T. Nilges, M. Bawohl, S. Lange, *Z. Naturforsch. B* **2007**, *62*, 955–964.

[20] T. Nilges, J. Messel, M. Bawohl, S. Lange, *Chem. Mater.* **2008**, *20*, 4080–4091.

[21] S. Lange, M. Bawohl, T. Nilges, *Inorg. Chem.* **2008**, *47*, 2625–2633.

[22] F. Baumer, T. Nilges, *Inorg. Chem.* **2017**, *56*, 13930–13937.

[23] A. Vogel, T. Miller, C. Hoch, M. Jakob, O. Oeckler, T. Nilges, *Inorg. Chem.* **2019**, *58*, 6222–6230.

[24] A. Vogel, T. Nilges, *Inorg. Chem.* **2021**, *60*, 15233–15241.

[25] T. Nilges, M. Bawohl, O. Osters, S. Lange, J. Messel, *Z. Phys. Chem.* **2010**, *224*, 1505–1531.

[26] U. Schürmann, V. Duppel, T. Nilges, S. Britvin, V. A. Kovalenker, L. Kienle, *Z. Anorg. Allg. Chem.* **2013**, *639*, 2761–2766.

[27] C. Manolikas, J. Spyridelis, *Mater. Res. Bull.* **1977**, *12*, 907–913.

[28] H. Jang, Y. S. Jung, M.-W. Oh, *Heliyon* **2023**, *9*, e21117.

[29] M. Z. Akgul, G. Konstantatos, *ACS Appl. Nano Mater.* **2021**, *4*, 2887–2894.

[30] F. N. Guild, *Econ. Geol.* **1917**, *12*, 297.

[31] A. J. Frueh Jr, *Z. Kristallogr.* **1954**, *106*, 299–307.

[32] S. N. Guin, D. Sanyal, K. Biswas, *Chem. Sci.* **2016**, *7*, 534–543.

[33] J. Le Roy, J. Moreau, G. Brun, B. Liautard, *J. Alloys Compd.* **1992**, *186*, 249–254.

[34] M. Bawohl, *Dissertation*, Universität Münster **2010**.

[35] B. Owens-Baird, P. Yox, S. Lee, X. B. Carroll, S. Grass Wang, Y.-S. Chen, O. I. Lebedevc, K. Kovnir, *Chem. Sci.* **2020**, *11*, 10255–10264.